



HAL
open science

Experimental study of boiling in porous media

Paul Sapin, Paul Duru, Florian Fichot, Marc Prat, Michel Quintard

► **To cite this version:**

Paul Sapin, Paul Duru, Florian Fichot, Marc Prat, Michel Quintard. Experimental study of boiling in porous media. ASME 2013 Heat Transfer Summer Conference, Jul 2013, Minneapolis, United States. pp.0. hal-04086559

HAL Id: hal-04086559

<https://hal.science/hal-04086559>

Submitted on 2 May 2023

HAL is a multi-disciplinary open access archive for the deposit and dissemination of scientific research documents, whether they are published or not. The documents may come from teaching and research institutions in France or abroad, or from public or private research centers.

L'archive ouverte pluridisciplinaire **HAL**, est destinée au dépôt et à la diffusion de documents scientifiques de niveau recherche, publiés ou non, émanant des établissements d'enseignement et de recherche français ou étrangers, des laboratoires publics ou privés.



Open Archive TOULOUSE Archive Ouverte (OATAO)

OATAO is an open access repository that collects the work of Toulouse researchers and makes it freely available over the web where possible.

This is an author-deposited version published in : <http://oatao.univ-toulouse.fr/>
Eprints ID : 10283

To link to this article : doi:10.1115/HT2013-17262
URL : <http://dx.doi.org/10.1115/HT2013-17262>

<p>To cite this version : Sapin, Paul and Duru, Paul and Fichot, Florian and Prat, Marc and Quintard, Michel Experimental study of boiling in porous media. (2013) In: ASME 2013 Heat Transfer Summer Conference, 14 July 2013 - 19 July 2013 (Minneapolis, United States).</p>
--

Any correspondence concerning this service should be sent to the repository administrator: staff-oatao@listes-diff.inp-toulouse.fr

EXPERIMENTAL STUDY OF BOILING IN POROUS MEDIA

Paul Sapin*

Université de Toulouse ; INPT, UPS;
IMFT (Institut de Mécanique des Fluides de Toulouse) ;
Allée Camille Soula,
F-31400 Toulouse, France
Email: psapin@imft.fr

Paul Duru

Université de Toulouse ; INPT, UPS;
IMFT (Institut de Mécanique des Fluides de Toulouse) ;
Allée Camille Soula,
F-31400 Toulouse, France

Florian Fichot

Institut de Radioprotection et de Sécurité Nucléaire (IRSN)
Division of Major Accidents Prevention
BP 3, 13115 St Paul lez Durance, France.

Marc Prat

Michel Quintard
Université de Toulouse ; INPT, UPS;
IMFT (Institut de Mécanique des Fluides de Toulouse) ;
Allée Camille Soula,
F-31400 Toulouse, France
and CNRS ; IMFT ; F-31400 Toulouse, France.

ABSTRACT

Following a long-lasting failure in the cooling system of a pressurized water reactor (PWR), the superheated core can be efficiently cooled down by reflooding. The macroscopic model used at the French Institute of Radioprotection and Nuclear Safety (IRSN) to simulate this process is based on strong assumptions on the microscopic flow patterns. This paper describes the experimental setup designed for the study of boiling in porous media with the emphasis on various pore-scale boiling regimes. The final experimental setup is a two-dimensional porous medium made of 392 cylinders randomly placed between two ceramic plates. Each heating cylinder is a RTD probe (Resistance Temperature Detector), that can give thermal measurements in every point of the test section as well as heat generation. This paper presents preliminary results: pool boiling is characterized for a single cylinder mounted in the test section and reflooding of a line of 9 cylinders is observed.

NOMENCLATURE

g	Standard gravity, m^2/s
h	Volumetric heat transfer coefficient, $W/m^3/K$
h_β	Averaged specific enthalpy of the β phase, J/kg
h_β^{sat}	Specific enthalpy of saturated β phase, J/kg
I	Electric intensity, A
J	Leverett function
K	Macroscopic permeability, m^2
$k_{r\beta}$	Relative permeability of the β phase
\mathbf{K}_β^*	Effective thermal dispersion tensor, $W/m/K$
L_{cap}	Capillary length, m
\dot{m}	Evaporation rate, $kg/m^3/s$
p_β	Averaged pressure of the β phase, Pa
Q	Volumetric heat flux, W/m^3
R	Electric resistance, Ω
T	Temperature, K
T_β	Averaged temperature of the β phase, K
ΔT_{sat}	Wall superheat: $T_w - T_{sat}$, K
v_β	Averaged speed in the β phase, m/s

*Address all correspondence to this author.

Greek symbols

α	Void fraction or gas saturation
ε	Porosity
η	Macroscopic passability, m
$\eta_{r,\beta}$	Relative passability of the β phase
μ_β	Viscosity of the β phase, Pa · s
ρ	Density, kg / m ³
σ	Surface tension, N / m
θ	Contact angle
ω_s	Volumetric thermal source, W / m ³

Subscripts

cv	Convective exchange
g	Gas phase
i	Interface
l	Liquid phase
nb	Nucleate boiling
s	Solid phase
sat	Saturation
w	Wall
β	Phase index: $\beta = g, l, s$

INTRODUCTION

In a pressurized water reactor (PWR) in nominal operating range, the thermal energy generated by the fission of atoms is transferred to the flowing water. Following a long-lasting failure in the cooling system and despite the lowering of the control rods, the residual power induces water evaporation, which leads to the drying and the degradation of the fuel rods. The nuclear accidents which occurred in one reactor at the Three Mile Island nuclear power plant in 1979 and more recently in three reactors at the Fukushima Daiichi power station have shown that this cooling malfunction can lead to the melting of the core materials. The fragmentation of the resulting molten corium forms a hot debris bed, comparable to a heat-generating porous medium. The successive stages of a LOCA (Loss of Coolant Accident) scenario and the resulting debris bed have been characterized experimentally thanks to the Phebus PF setup (1:5000 scale) [1] and to the observations on the TMI-2 reactor. Provided a water source is available, the particle bed can efficiently be cooled down by reflooding. This will in general involve intense boiling mechanisms that must be modeled properly in order to evaluate the coolability of a degraded core. The coolability of debris bed has been studied experimentally and theoretically in the last 35 years, notably at the IRSN, so as to estimate the increase of pressure in the primary cooling circuit, the hydrogen production and the release of fission products.

The PRELUDE experimental setup (Fig. 1(a)) has been developed at the IRSN to study the reflooding of a bed of steel balls, heated by induction. The size of these steel particles (from 2 to

8 mm diameter) has been chosen in agreement with the observations of the TMI-2 reactor. The tests performed on this experimental device allowed a local thermal non-equilibrium macroscopic model to be validated. Many theoretical works [2] and experimental observations (PRELUDE experiments) suggest that several boiling and evaporation regimes at the pore scale may impact the macroscopic properties of the model required to simulate properly the available experiments.

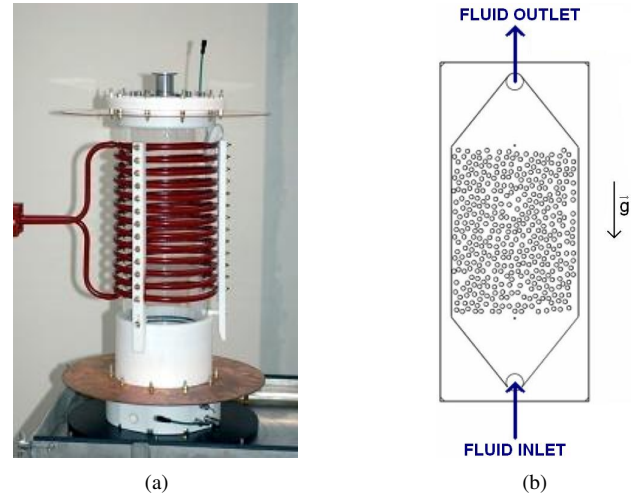


FIGURE 1. (a) PRELUDE EXPERIMENTAL SETUP; (b) TWO-DIMENSIONAL MODEL POROUS MEDIUM.

This paper describes preliminary experimental results for boiling in porous media with the emphasis on various pore-scale boiling regimes. The experimental setup (Fig. 1(b)) is a two-dimensional porous medium made of cylinders randomly placed between two ceramic plates. The heat is generated by the Joule effect, each of the cylinders being a heating element controlled individually. This allows us not to heat up all the cylinders, which reproduces more faithfully the situation in a reactor core where only the fuel fragments release thermal energy.

PREVIOUS STUDIES

Flows and heat transfer with phase-change in porous media are studied for various application domains: drying problems [3], heat exchangers [4], geothermal energy systems [5] and nuclear safety [6] [7]. For the latter, understanding of the reflood of a heat-generating debris bed is crucial. Different kinds of modelization able to describe this phenomenon are present in the literature : models based on entropy balance [8], pore network models [9] and macroscopic models using the method of volume averaging [10].

A macroscopic model [2, 7, 11] has been developed for the ICARE/CATHARE code of the IRSN for safety analysis of PWRs, using the method of volume averaging. In this model, local thermal non-equilibrium between the three phases (solid, liquid, gas) is considered. The macroscopic equations are derived for each phase from the microscopic problems. With the quasi-static hypothesis, which means that the impact of the gas-liquid interface speed in the up-scaling problem is neglected, the momentum balance equations are equivalent to generalized Darcy's laws for each fluid phase, with Forchheimer terms accounting for inertial effects (Eqn. (1) and (2)) :

$$\alpha \rho_g \left(\frac{\partial \mathbf{v}_g}{\partial t} + \mathbf{v}_g \cdot \nabla \mathbf{v}_g \right) = \alpha \nabla p_g + \alpha \rho_g \mathbf{g} - \varepsilon \alpha^2 \left(\frac{\mu_g}{K k_{rg}} \mathbf{v}_g + \varepsilon \alpha \frac{\rho_g}{\eta \eta_{rg}} \mathbf{v}_g |\mathbf{v}_g| \right) \quad (1)$$

$$(1 - \alpha) \rho_l \left(\frac{\partial \mathbf{v}_l}{\partial t} + \mathbf{v}_l \cdot \nabla \mathbf{v}_l \right) = (1 - \alpha) \nabla p_l + (1 - \alpha) \rho_l \mathbf{g} - \varepsilon (1 - \alpha)^2 \left(\frac{\mu_l}{K k_{rl}} \mathbf{v}_l + \varepsilon (1 - \alpha) \frac{\rho_l}{\eta \eta_{rl}} \mathbf{v}_l |\mathbf{v}_l| \right) \quad (2)$$

In these equations, p_β , ρ_β and \mathbf{v}_β are respectively the macroscopic pressure, density and velocity of the β -phase ($\beta=g,l$ for gas and liquid). For spherical particle beds, as used in the PRELUDE experimental setup, the intrinsic permeability K and passability η are respectively calculated thanks to the Carman-Kozeny relation [12] and the Ergun law [13]. The relative permeability $k_{r\beta}$ and passability $\eta_{r\beta}$ are obtained with the Brooks-Corey relations [14]. The capillary pressure, modeled as a function of saturation, is introduced in the equations to account for the effects of pressure between the wetting and the non-wetting phases :

$$p_c = p_g - p_l = \sigma \cos \theta \sqrt{\frac{\varepsilon}{K}} J(S) \quad (3)$$

where J is the Leverett function, expressed as a function of saturation in the macroscopic model according to Turland-Moore relation [15].

As for the heat transfer problem, the up-scaling of the micro-scale mass and energy balance equations leads to the establishment of the macro-scale energy balance equations relative to each phase (Eqn. (4),(5),(6)):

$$\frac{\partial (\alpha \varepsilon \rho_g h_g)}{\partial t} + \nabla (\alpha \varepsilon \rho_g \mathbf{v}_g h_g) = \nabla (\mathbf{K}_g^* \cdot \nabla T_g) + \dot{m}_g h_g^{sat} + Q_{sg} + Q_{gi} \quad (4)$$

$$\frac{\partial ((1 - \alpha) \varepsilon \rho_l h_l)}{\partial t} + \nabla ((1 - \alpha) \varepsilon \rho_l \mathbf{v}_l h_l) = \nabla (\mathbf{K}_l^* \cdot \nabla T_l) + \dot{m}_l h_l^{sat} + Q_{sl} + Q_{li} \quad (5)$$

$$\frac{\partial ((1 - \varepsilon) \rho_s h_s)}{\partial t} = \nabla (\mathbf{K}_s^* \cdot \nabla T_s) - Q_{sl} - Q_{sg} - Q_{si} + \bar{\omega}_s \quad (6)$$

where h_β and T_β represent respectively the macro-scale enthalpy and temperature of the β -phase ($\beta=g,l,s$ for gas, liquid and solid). The macroscopic coefficients involved in these equations are the effective thermal dispersion tensors \mathbf{K}_β^* and the thermal coefficients $h_{s\beta}$ and $h_{\beta i}$ used in the definitions of thermal exchanges between phases $Q_{s\beta}$ and $Q_{\beta i}$ (Eqn. (7) and (8)) :

$$Q_{\beta i} = h_{\beta i} (T_\beta - T_{sat}) \quad (7)$$

$$Q_{s\beta} = h_{s\beta} (T_s - T_\beta) \quad (8)$$

These macroscopic coefficients may be calculated by solving the closure problems provided by averaging processes. They have been determined analytically for simple configurations [16] (stratified and Chang cells), still under the quasi-static hypothesis. The gas-liquid interface being considered stationary, these models allow the heat exchanges to be described properly only for evaporation or condensation of a fluid film without nucleation. As a result, the heat exchanges are underestimated in the nucleate, transition and film boiling regimes, encountered during a core reactor reflood.

Bachrata *et al.* [17] propose an improvement of this model. For the film boiling regime, a modified version of the Berenson's correlation [18] is used to estimate local heat transfer. In the transition boiling region, the local wall-to-fluid heat flux is estimated as a function of the critical heat flux (CHF), itself calculated with the CATHARE correlation [19] based on Groeneveld table [20]. As for the nucleate boiling regime, the local heat transfer coefficient h is computed by adding the nucleate boiling h_{nb} (obtained with Thom's correlation [21]) and forced convection h_{cv} (obtained with Dittus-Boelter correlation [22]) contributions, weighted by a factor depending on void fraction:

$$h = (1 - \alpha^n) h_{nb} + ((1 - \alpha) h_{cv,l} + \alpha h_{cv,g}) \quad (9)$$

where the coefficient n is determined thanks to the experimental results from PRELUDE.

The correlations for boiling in convective flows heat transfer coefficient proposed in the literature can be classified in three categories [23] : the summation models [24], the asymptotic models [25] and models based on flow patterns [26]. The heuristic model proposed by Bachrata *et al.* [17] is similar to Chen's summation model [24]. No correlation being available for boiling in porous media, and in the light of the comparison with experimental results, this modeling seems to be on the right track.

However, this kind of correlation has been developed for macroscopic boiling while microscopic boiling can be encountered in the considered porous media, regardless of the chosen macro-to-micro criterion [23]. Besides, the interaction between heating elements in a porous medium makes the coalescence of bubbles easier, which might in particular influence the CHF value. LITER and Kaviany [4] have indeed shown the improvement of porous-layer coatings on the predicted CHF value, both theoretically and experimentally ; Chai and Wen [27] have conducted a theoretical analysis on boiling peak heat flux with porous media, showing the influence of porous coatings thickness and porosity on the CHF.

It is then essential to obtain pore-scale visualizations and local thermal measurements (heat flux / temperature) for boiling in porous media, in order to identify the flow patterns and the heat transfer processes (nucleation, convection, film evaporation...). From there, it will be possible to propose macroscopic correlations incorporating more precisely the physics at the pore scale.

EXPERIMENTAL SETUP

The experimental setup designed for the study of boiling in porous medium (test section) is a closed loop circuit (Fig. 2).

A gear pump (flow rate from 2 to 100mL/min) circulates the fluid, the temperature of which is brought close to the saturation temperature before the test section inlet. The vapor created by the boiling processes is then condensed. A tank is used as a plenum chamber to trap non condensed vapor and the remaining non condensable gases (air principally). The operating fluid is a fluorinert : the 3M™ Novec™ Engineered Fluid HFE-7000. It is indeed convenient for our study for many reasons: its low saturation temperature ($T_{sat} = 34^\circ\text{C}$ at a pressure of 1atm) allows all the boiling regimes to be observed with moderate thermal constraints; and it is a low-toxicity, non-flammable and dielectric fluid, which ensures safety during the manipulations. It is nonetheless important to avoid prolonged contact with air since the HFE-7000 is highly volatile and has a non-negligible global warming potential (370 for a 100-year integrated time horizon). For that reason and in order to avoid the presence of air within the circuit (which would significantly reduce the saturation temperature of the fluid), the filling process is handled by vacuum. The HFE-7000 fluid is highly hydrophilic, as is water. Its contact angle with ceramics is thus close to 0° , as it is theoretically the case for water in contact with bare metal or ceramic surfaces. As regards the capillary effects, the water surface tension (58.8mN/m at 100°C) is approximately 4.7 times higher than the HFE-7000 surface tension at the saturation temperature (12.4mN/m at 34°C). So, the capillary length L_{cap} , defined in the equation (10), is 2.6 times higher for water than for the fluorinert.

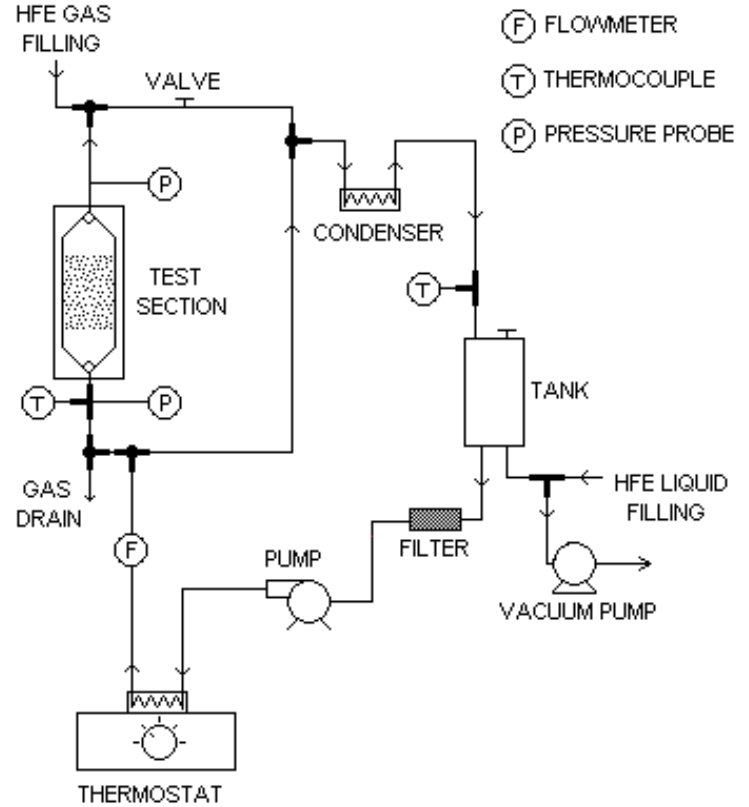


FIGURE 2. EXPERIMENTAL SETUP: CLOSED FLUID CIRCUIT.

$$L_{cap} = \sqrt{\frac{\sigma}{\rho g}} \quad (10)$$

The test section is a two-dimensional porous medium made of 392 cylinders randomly placed between two ceramic plates, one of which is transparent (Fig. 3). The PRELUDE experiments aim to study the reflooding of particle beds made of steel balls, the diameters of which range between 2 and 8 mm. Given the difference between the capillary lengths, the diameter of the heating cylinders has been chosen to be 2 mm, so that the capillary effects in this experimental setup are representative of those obtained with the previous experiments.

Each cylinder is a Resistance Temperature Detector (RTD), not only used as a heating element but also as a local temperature and heat flux sensor. A RTD element (Fig. 4) consists of a length of fine coiled wire wrapped around an insulating core, sealed in a ceramic coating. Since the platine resistance changes with temperature (100Ω at 0°C for the used PT100 probes), one can easily measure the temperature.

It is then also necessary to provide a heat flux control module for the heating cylinders because of this change in resistance

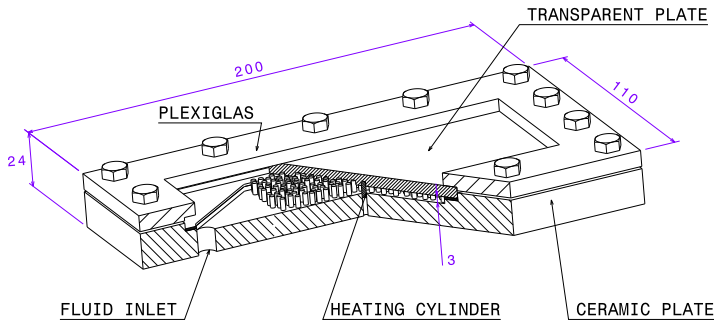


FIGURE 3. EXPERIMENTAL SETUP: TEST SECTION (DIMENSIONS IN mm).

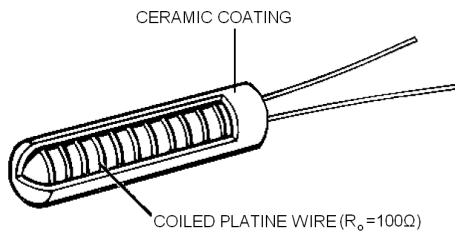


FIGURE 4. RTD ELEMENT

(Joule effect depending on $R(T)$). So each probe is linked to a microelectronic servo-control system, able to control and measure in real time the heat flux transmitted to the element as well as its temperature. This allows precise measurements near the CHF or near the Leidenfrost temperature, with the aim in mind to provide new Nukiyama's curves. Thanks to a simple heat conduction analysis of the ceramic coating, the response time of these probes is evaluated to be 1 s. This time delay is non-negligible in comparison to the timing of transition between film and nucleate boiling regimes observed in the reflooding example presented later in this paper (from 4 to 12 s). However, in order to provide Nukiyama's curves in the porous medium, established boiling regimes are considered, so the impact of this time delay is much less problematic for these measurements.

The upper plate being transparent, visualization provides the phase distribution within the porous medium. Camera acquisition together with the thermal measurements allow us to describe the effective heat exchange according to the observed boiling regime.

The heat flux or temperature control command is given to each module via a computer. The servo-control systems are then autonomous. In this way, only the desired probes are linked to the computer to acquire thermal measurements in real-time (Fig. 5).

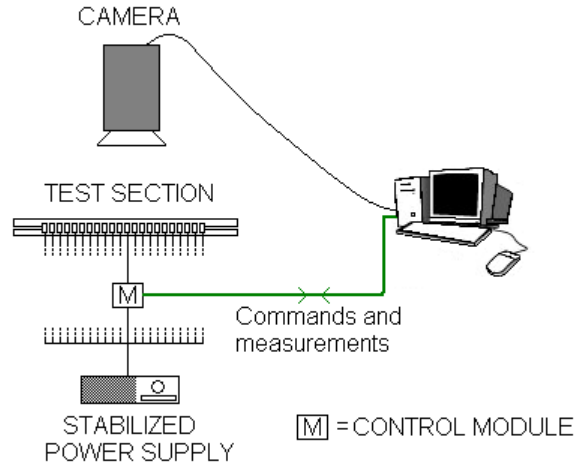


FIGURE 5. DATA ACQUISITION

RESULTS

A preliminary test section with one isolated heating element as well as 9 cylinders in line has been designed for studying boiling on a unique horizontal cylinder and the reflood process of a heated row. As a first step, the thermal resistance of the probe ceramic coating has to be determined (Fig. 4). For the temperature measurement with RTD probes, an usual problem is to avoid self-heating (low current is used), because this leads to a temperature difference between the cylinder wall temperature and the platine wire temperature effectively measured. Since self-heating is used in our experiment as the power source, this temperature difference must be known at every time. That is why ceramic coating resistances have been measured thanks to infrared thermography for different thermal equilibriums (around 30 K/W).

Subcooled Pool Boiling on a horizontal cylinder

Once this correction is applied, pool boiling around a cylinder has been studied. By controlling the imposed heat flux, the main boiling regimes have been observed. A Nukiyama's curve (Fig. 6) has been obtained to characterize pool boiling on the used RTD elements horizontally placed in the test section in a HFE-7000 bath at 20°C. The assembly of the heating element between the two ceramic plates has been modeled in COMSOL Multiphysics. Thanks to a heat conduction model, with natural convection in air on external boundaries and convective heat exchange on internal boundaries, and thanks to the thermal measurements, the heat loss and the effectively transmitted heat fluxes have been obtained by iteration, playing with the value of the internal convective heat transfer coefficient.

During the increase in heat flux, nucleate boiling with isolated vapor bubbles (Fig. 8(a)) and then with the formation of vapor pockets (Fig. 8(b)) are observed on the element. Below

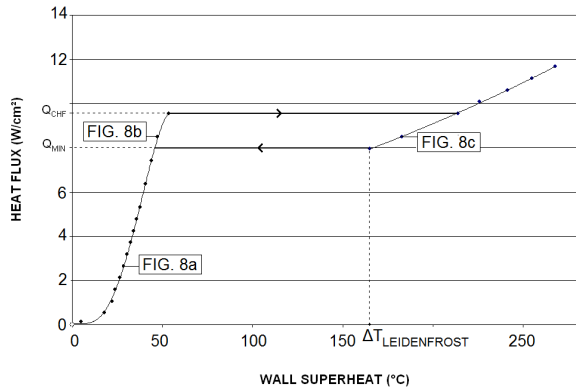


FIGURE 6. NUKIYAMA'S CURVE FOR HFE-7000 BOILING ON A HORIZONTAL CYLINDER

the critical heat flux ($Q_{CHF} = 9.5 \text{ W/cm}^2$), the liquid remains in contact with the heating cylinder wall despite the coalescence of bubbles. The heat exchange reaches a maximum just before the burnout point, at which a vapor film is formed at the heater surface. The so-called boiling crisis is violent and leads to an increase in wall superheat (of approximately 160 K) and an important reduction in the heat transfer rate. The film boiling regime (Fig. 8(c)) is maintained while decreasing the heat flux: the vapor film thickness decreases until the heat flux reaches a minimum at the so-called Leidenfrost point, for which $\Delta T_{sat} = 162 \text{ K}$ and $Q_{MIN} = 8 \text{ W/cm}^2$.

The official CHF given by 3MTM society is however 18 W/cm^2 from a horizontal 0.5 mm diameter platinum wire in a quiescent pool of saturated fluid. The difference with the value found here can be explained in part by the scaling effects. Indeed, using the Lienhard's correlations for pool boiling on finite bodies [28], and taking into account the effects of subcooling, the theoretical CHF for a 2 mm diameter horizontal cylinder is found to be 14.3 W/cm^2 . The remaining difference is therefore due to a confinement effect: the cylinder is indeed placed between two plates spaced of 3 mm , which facilitates the coalescence of gas bubbles.

The heat transfer coefficients for both the nucleate and the film boiling regimes have been computed. Their evolutions as a function of the transferred heat flux is shown in Fig. 7.

Figure 8(c) shows a film boiling regime on a 2 mm diameter horizontal cylinder. This picture is less sharp than the images in Fig. 8(a) and Fig. 8(b) because of the difficulty to capture the gas-liquid interface. The generation of vapor slugs in this regime is however well brought into focus. The behavior of these slugs in a heated porous medium is hardly predictable (coalescence with other slugs or vapor films, simple Taylor bubbles...) for a large number of pores. It will thus be very instructive to observe how the confinement affects the boiling and convective heat exchanges. This is why we had to study boiling on a cylinder

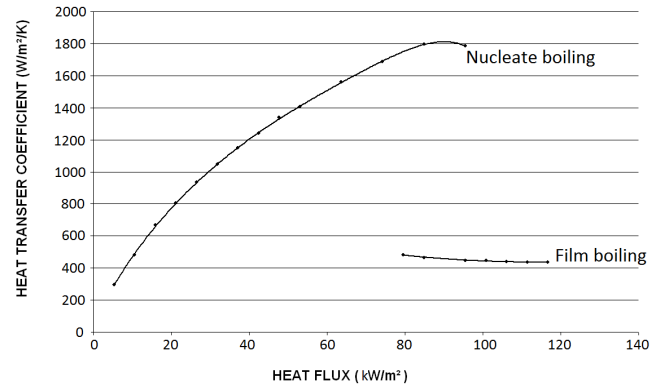


FIGURE 7. HEAT TRANSFER COEFFICIENT VS HEAT FLUX FOR HFE-7000 BOILING ON A HORIZONTAL CYLINDER

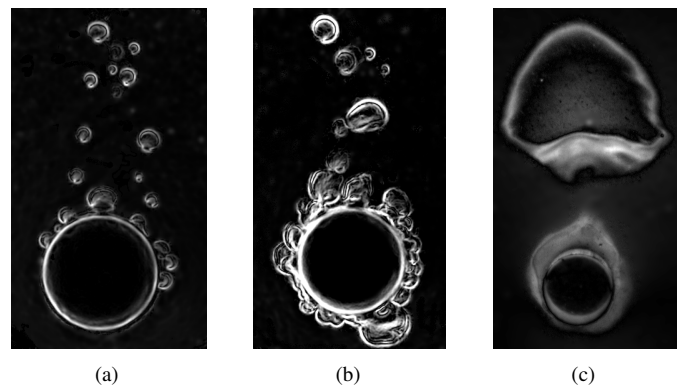


FIGURE 8. (a) Partial nucleate boiling; (b) Intense nucleate boiling; (c) Film boiling.

mounted in the test section: the aim was not the study of boiling on horizontal cylinders, but rather to characterize precisely the behavior of an isolated heating element.

Reflooding of a superheated line of cylinders

The second preliminary experiment is the observation of the reflow of 9 horizontal cylinders in line, superheated at a temperature of approximately 200°C , obtained with an effective heat flux of 4 W/cm^2 that will be maintained constant for the nine heaters during the reflowing, regardless of the temperature. The HFE-7000 liquid is injected at 20°C and 0.2 cm/s . The thermal measurements during the reflow process are presented in Figure 9. The indexes on the curves refer to Figure 10.

The initial wall temperature of the probes is superior to the obtained Leidenfrost temperature, the first observed regime is therefore the film boiling regime. But the effective heat flux transferred to each cylinder is inferior to the minimum heat flux, so the vapor films cannot be maintained, especially with the in-

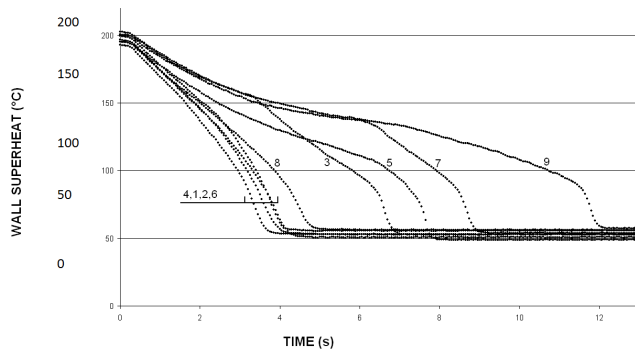


FIGURE 9. EVOLUTION OF THE SUPERHEATED CYLINDERS TEMPERATURES DURING THE REFLOOD

fluence of superposed flow. The steady-state regime is thus the nucleate boiling regime. The transition between the two regimes is observed by a slope break in the cool-down curve for each cylinder. The study of the transition boiling regime will be undertaken later with temperature control.

One can notice differences between the cool-down curves. Indeed the film-to-nucleate boiling regime transition happens at various times for the cylinders. This can be due to the high turbulence taking place after the boiling front: the dynamics of bubble detachment is highly influenced by the recirculation. However, by repeating the operation, it has been observed that the cooling of probes 5,7,8 and 9 is always delayed in comparison to the others, even after changing the probes. This lets us think of a problem in the horizontality of the test section. This problem will not occur with the final experimental setup since the cylinders are randomly placed. Figure 10 shows the generated gas bubbles during the reflooding, 6.4s after the liquid front contact with superheated cylinders. Only the ninth probe remains in film boiling at that time, which is in accordance with the corresponding thermal measurements.

By increasing the rod spacing, the results would be inappreciably affected because the current spacing (5mm) is already significantly higher than the typical bubble departure diameter. However, by decreasing this spacing, coalescence of bubbles from different cylinders may happen more frequently, which would help the film boiling regime to be maintained. This is what we expect to observe in the final experimental setup.

CONCLUSION

These preliminary experiments have validated many experimental settings and have shown the feasibility of the project. The results already obtained give us precious informations for boiling of HFE-7000 in our specific configuration. This will help us for the interpretation of results in porous media. The experiments with the two-dimensional porous medium will be conducted, so

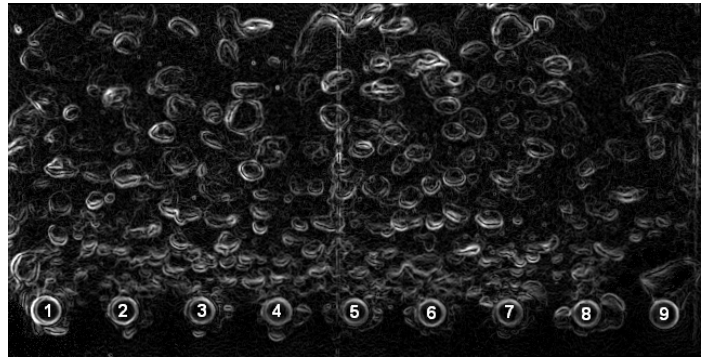


FIGURE 10. Intense nucleate boiling for cylinders 1 to 8 and film boiling for cylinder 9.

“Nukiyama’s curves for porous medium” will be presented at the HT2013 conference. Many questions still need to be answered, for example the impact of a partial heating (one out of two cylinders heated) on the heat exchange.

Parallel to the experimental work, a stability analysis is also carried out to assess the potential destabilization of the vaporization front.

ACKNOWLEDGMENT

Thanks go to H. Ayroles and R. Soeparno for all the time they spent on the experimental setup development.

REFERENCES

- [1] Jacquemain, D., Bourdon, S., de Braemaeker, A., and Bar-rachin, M., 2000. “Phebus fpt1 final report”. *Document PHÉBUS PF*.
- [2] Petit, F., Fichot, F., and Quintard, M., 1999. “Écoulement diphasique en milieu poreux: modèle à non-équilibre local”. *International journal of thermal sciences*, **38**(3), pp. 239–249.
- [3] Prat, M., 1991. “2d modelling of drying of porous media: influence of edge effects at the interface.”. *Drying technology*, **9**(5), pp. 1181–1208.
- [4] Liter, S. G., and Kaviany, M., 2001. “Pool-boiling CHF enhancement by modulated porous-layer coating: theory and experiment”. *International Journal of Heat and Mass Transfer*, **44**(22), Nov., pp. 4287–4311.
- [5] Woods, A. W., 1999. “Liquid and vapor flow in superheated rocks”. *Annual Review of Fluid Mechanics*, **31**(1), pp. 171–199.
- [6] Lipinski, R., 1984. “A coolability model for postaccident nuclear reactor debris”. *Nucl. Technol.:(United States)*, **65**(1).
- [7] Fichot, F., Duval, F., Trégourès, N., Béchaud, C., and Quin-

- tard, M., 2006. "The impact of thermal non-equilibrium and large-scale 2D/3D effects on debris bed reflooding and coolability". *Nuclear Engineering and Design*, **236**, Oct., pp. 2144–2163.
- [8] Bénard, J., Eymard, R., Nicolas, X., and Chavant, C., 2005. "Boiling in porous media: Model and simulations". *Transport in Porous Media*, **60**(1), pp. 1–31.
- [9] Yiotis, A. G., Tsimpanogiannis, I. N., Stubos, A. K., and Yortsos, Y. C., 2006. "Pore-network study of the characteristic periods in the drying of porous materials". *Journal of Colloid and Interface Science*, **297**(2), pp. 738 – 748.
- [10] Whitaker, S., 1999. *The method of volume averaging*, Vol. 13. Springer Netherlands.
- [11] Duval, F., Fichot, F., and Quintard, M., 2004. "A local thermal non-equilibrium model for two-phase flows with phase-change in porous media". *International Journal of Heat and Mass Transfer*, **47**(3), pp. 613–639.
- [12] Carman, P. C., 1937. "The determination of the specific surface area of powder I". *J. Soc. Chem. Ind.*, **57**, pp. 225–234.
- [13] Ergun, S., 1952. "Fluid flow through packed columns". *Chem. Eng. Prog.*, **48**.
- [14] Brooks, R. H., and Corey, A. T., 1966. "Properties of porous media affecting fluid flow". *J. Irrig. Drain. Div. Am. Soc. Civ. Eng. IR2*, **92**, pp. 61–89.
- [15] Turland, B. D., and Moore, K., 1983. "Debris bed heat transfer with top and bottom cooling". *AIChE Symp. Ser.*, **79**, p. 256267.
- [16] Duval, F., 2002. "Modélisation du renoyage d'un lit de particules: contribution à l'estimation des propriétés de transport macroscopiques". PhD thesis, Institut National Polytechnique de Toulouse.
- [17] Bachrata, A., Fichot, F., Repetto, G., Quintard, M., and Fleurot, J., 2011. "Quench front progression in a superheated porous medium : Experimental analysis and model development". In NURETH-14.
- [18] Berenson, P. J., 1961. "Film-boiling heat transfer from a horizontal surface". *Journal of Heat Transfer (U.S.)*, **83**.
- [19] Chikhi, N., and Fichot, F., 2010. "Reflooding model for quasi-intact rod configuration: Quench front tracking and heat transfer closure laws". *Nuclear Engineering and Design*, **240**(10), Oct., pp. 3387–3396.
- [20] Groeneveld, D. C., Cheng, S. C., and Doan, T., 1986. "AECL-UO critical heat flux lookup table". *Heat Transfer Engineering*, **7**(1-2), pp. 46–62.
- [21] Thom, J., Walker, W., Fallon, T., and Reising, G., 1966. "Boiling in subcooled water during flow up hasted tubes or annuli". *Proc. Inst. Mech. Eng.*, **180**, pp. 226–246.
- [22] Dittus, F. W., and Boelter, L. M. K., 1930. *Heat Transfer in Automobile Radiators of the Tubular Type*. University of California Press.
- [23] Thome, J. R., 2004. "Boiling in microchannels: a review of experiment and theory". *International Journal of Heat and Fluid Flow*, **25**(2), pp. 128–139.
- [24] Chen, J., 1966. "Correlation for boiling heat transfer to saturated fluids in convective flows". *I&EC Process Design and Development*, **5**(3), July, pp. 322–329.
- [25] Steiner, D., and Taborek, J., 1992. "Flow boiling heat transfer in vertical tubes correlated by an asymptotic model". *Heat transfer engineering*, **13**(2), pp. 43–69.
- [26] Thome, J. R., Dupont, V., and Jacobi, A. M., 2004. "Heat transfer model for evaporation in microchannels. part i: presentation of the model". *International Journal of Heat and Mass Transfer*, **47**(14-16), July, pp. 3375–3385.
- [27] Chai, L., and Wen, D., 2005. "Theoretical analyses on boiling critical heat flux with porous media". *Heat and Mass Transfer*, **41**(9), pp. 780–784.
- [28] Lienhard, J. H., and Dhir, V. K., 1973. "Hydrodynamic prediction of peak pool-boiling heat fluxes from finite bodies". *Journal of Heat Transfer*, **95**(2), May, pp. 152–158.